Black Objects and Hoop Conjecture in Five-dimensional Space-time

Hisa-aki Shinkai, and Yuta Yamada

Faculty of Information Science and Technology, Osaka Institute of Technology, Hirakata, Osaka 573-0196, Japan

Abstract

We numerically investigated thin ring in five-dimensional spacetime, both of the sequences of initial data and their initial time evolution. Regarding to the initial data, we modeled the matter in non-rotating homogeneous toroidal configurations under the momentarily static assumption, solved the Hamiltonian constraint equation, and searched the apparent horizon. We discussed when S^3 (black hole) or $S^1 \times S^2$ (black ring) horizons ("black objects") are formed. By monitoring the location of the maximum Kretchmann invariant, an appearance of 'naked singularity' or 'naked ring' under the special situations is suggested. We also discuss the validity of the hyper-hoop conjecture using minimum area around the object.
We also show initial few time evolutions under the maximal time slicing condition, expressing the matter with collisionless particles. We found the dynamical behaviors are different depending on the initial ring radius.

1 Introduction

In higher dimensional general relativity(GR), there are two interesting problems. One is the cosmic censorship hypothesis (CCH) originally proposed in $3+1$ dimensional GR. CCH states collapse driven singularities will always be clothed by event horizon and hence can never be visible from the outside. By contrast, *hyper-hoop* conjecture[1] states that black holes will form when and only when a mass M gets compacted into a region whose $(D-3)$ dimensional area V_{D-3} in every direction is $V_{D-3} \leq G_D M$. There are some semi-analytic studies(e.g. [2]), but the validity and/or generality is unknown.

The other problem is stability of five-dimensional black-hole solutions. The four-dimensional black-holes are known to be S^2 from the topological theorem, while in higher-dimensional spacetime quite rich structures are available including "black ring(s)" [3]. There is, however, no confirmation for stability of such black-ring solutions.

In this report, we show the sequence of the initial data for the toroidal matter configurations. We investigate the validity of hyper-hoop conjecture by searching apparent horizons, and predict dynamics by evaluating the area of horizons[4]. Using the $4+1$ ADM formalism, we next show initial few steps of time evolutions of the initial data under the maximal time slicing condition.

2 Momentarily Static Black Ring Initial Data

2.1 The Hamiltonian constraint equation

We construct the initial data sequences on a four-dimensional space-like hypersurface. A solution of the Einstein equations is obtained by solving the Hamiltonian constraint equation if we assume the moment of time symmetry. We apply the standard conformal approach[5] to obtain the four-metric γ_{ij}. If we assume conformally flat trial metric $\hat{\gamma}_{ij}$, the equations would be simplified with a conformal transformation,

$$\gamma_{ij} = \psi^2 \hat{\gamma}_{ij} = \psi(X,Z)^2 (dX^2 + dZ^2 + X^2 d\vartheta_1 + Z^2 d\vartheta_2), \tag{1}$$

where $X = \sqrt{x^2+y^2}$, $Z = \sqrt{z^2+w^2}$, $\vartheta_1 = \tan^{-1}(y/x)$, and $\vartheta_2 = \tan^{-1}(z/w)$. By assuming ϑ_1 and ϑ_2 are the angle around the axis of symmetry, then the Hamiltonian constraint equation effectively becomes

$$\frac{1}{X}\frac{\partial}{\partial X}\left(X\frac{\partial \psi}{\partial X}\right) + \frac{1}{Z}\frac{\partial}{\partial Z}\left(Z\frac{\partial \psi}{\partial Z}\right) = -4\pi^2 G_5 \rho, \tag{2}$$

where ρ is the effective Newtonian mass density, G_5 is the gravitational constant in five-dimensional theory of gravity. We consider the cases with homogeneous toroidal matter configurations, described as

$$\left(\sqrt{x^2+y^2}-R_c\right)^2+\left(\sqrt{w^2+z^2}\right)^2 \le R_r^2, \tag{3}$$

where R_c is the circle radius of toroidal configuration, and R_r is the ring radius. This case is motivated from the "black ring" solution [3] though not including any rotations of matter nor of the spacetime. From obtained initial data, we also searched the location of an apparent horizon and the maximum value of the Kretchmann invariant $\mathcal{I}_{\max}$.

2.2 Definition of Hyper-Hoop

We also calculate hyper-hoop which is defined by two-dimensional area. We propose to define the hyper-hoop V_2 as a surrounding two-dimensional area which satisfies the local minimum area condition, $\delta V_2 = 0$. When the area of the spacetime outside the matter is expressed by the coordinate r, then $\delta V_2 = 0$ leads to the Euler-Lagrange type equation for $V_2(r, \dot{r})$. The hoop is expressed using $r = r_h(\phi)$ as

$$V_2^{(C)} = 4\pi \int_0^{\pi/2} \psi^2 \sqrt{\dot{r_h}^2 + r_h^2}\, r_h \cos\phi \, d\phi, \quad \text{or} \quad V_2^{(D)} = 4\pi \int_0^{\pi/2} \psi^2 \sqrt{\dot{r_h}^2 + r_h^2}\, r_h \sin\phi \, d\phi, \tag{4}$$

where $r = \sqrt{X^2+Z^2}$ and $\phi = \tan^{-1}(Z/X)$. $V_2^{(C)}$ expresses the surface area which is obtained by rotating respect to the Z-axis, while $V_2^{(D)}$ is the one with X-axis rotation. We also calculate hyper-hoop with $S^1 \times S^1$ topology for the toroidal cases, $V_2^{(E)}$,

$$V_2^{(E)} = 2\pi \int_0^{\pi} \psi^2 \sqrt{\dot{r_h}^2 + r_h^2}\,(r_h \cos\xi + R_c)\, d\xi, \tag{5}$$

where $r = \sqrt{(X-R_c)^2+Z^2}$ and $\xi = \tan^{-1}[Z/(X-R_c)]$.

2.3 Horizons and their area

Fig.1 shows two typical shapes of apparent horizons. We set the ring radius as $R_r/r_s = 0.1$ and search the sequence with changing the circle radius R_c. When R_c is less than $0.78 r_s$, we find that only the S^3-apparent horizon ("common horizon" over the ring) exists. On the other hand, when R_c is larger than $R_c = 0.78 r_s$, only the $S^1 \times S^2$ horizon ("ring horizon", hereafter) is observed.

We find that $\mathcal{I}_{\max}$ appears at the outside of matter configuration. Interestingly, $\mathcal{I}_{\max}$ is not hidden by the horizon when R_c is larger [see the case (c) of Fig.1]. Therefore, if the ring matter shrinks itself to the ring, then a "naked ring" (or naked di-ring) might be formed.

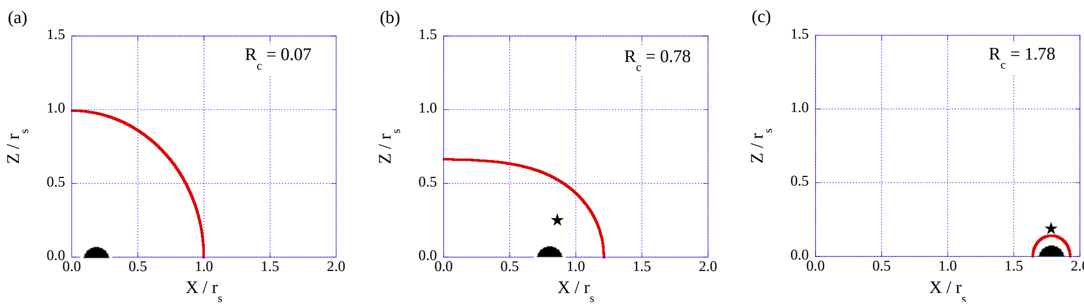

Figure 1: Matter distributions (shaded) and the location of the apparent horizon (line) for toroidal matter configurations. The asterisk indicates the location of the maximum Kretchmann invariant, $\mathcal{I}_{max}$.

We show the surface area of the apparent horizons A_3 left panel in fig.2. In left panel of fig.2, typical two horizons monotonically decrease with R_c/r_c, the largest one is when the matter is in the spheroidal one ($R_c/r_c = 0$). We also observe that the area of the common horizon is always larger than those of the ring horizon and both are smoothly connected in the plot. If we took account the analogy of the thermodynamics of black-holes, this suggest that the black-ring evolves to shrink its circle radius, and the ring horizon will switch to the common horizon at a certein radius.

Right panel in fig.2 shows the hyper-hoop $V_2^{(C)}$, $V_2^{(D)}$, and $V_2^{(E)}$. We plot the points where we found hyper-hoops. We note that $R_c/r_s = 0.78$ is the switching radius from the common horizon to the ring horizon, and that $V_2^{(C)}$ and $V_2^{(D)}$ are sufficiently smaller than unity if there is a common horizon. Therefore, hyper-hoop conjecture is satisfied for the formation of common horizon. On the other hand, for the ring horizon, we should consider the hoop $V_2^{(E)}$. In right panel of fig.2, in the region $R_c/r_s > 0.78$, $V_2^{(E)}$ exists only a part in this region and becomes larger than unity. Hence, for the ring horizon, the hyper-hoop conjecture is not a proper indicator. We conclude that the hyper-hoop conjecture is only consistent with the formation of common horizon as far as our definition of the hyper-hoop is concerned.

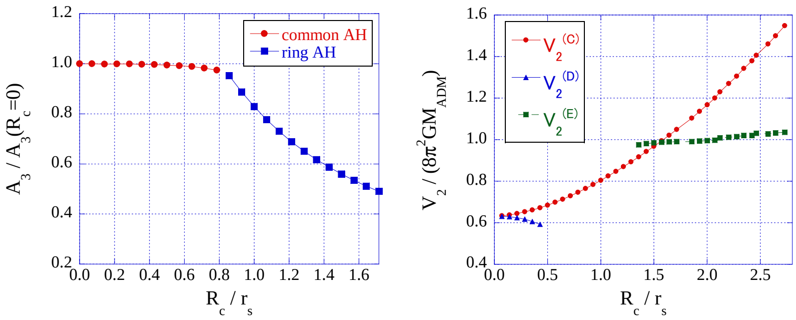

Figure 2: (Left) The area of the apparent horizon A_3. Plots are normalized by the area of spherical case ($R_c = 0$). We see both horizons' area are smoothly connected at $R_c/r_s = 0.78$, and both monotonically decrease with R_c/r_s. (Right) The ratio of the hyper-hoops V_2 to the mass M_{ADM} are shown for the sequence of Fig.1. The ratio less than unity indicates that the validity of the hyper-hoop conjecture.

3 Time Evolution of Toroidal Matter

We developed two numerical codes to follow the dynamics of five-dimensinal spacetime. The first code is fully 4+1 dimensional evolution code and the second is under the symmetry assumption of double axisymmetric space-time (both x- and z-rotational symmetry) using the Cartoon technique[7].

The gravitational field is integrated using the $4+1$ ADM formalism, of which evolution equations are written as

$$\frac{\partial \gamma_{ij}}{\partial t} = -2\alpha K_{ij} + D_i\beta_j + D_j\beta_i, \quad \text{and} \tag{6}$$

$$\begin{aligned}\frac{\partial K_{ij}}{\partial t} &= \alpha({}^{(4)}R_{ij} + KK_{ij}) - 2\alpha K_{il}K^{lj} - 12\pi^2\alpha(S_{ij} + \frac{1}{3}\gamma_{ij}(\rho - S)) \\ &\quad -D_iD_j\alpha + D_i\beta^m K_{mj} + D_j\beta^m K_{mi} + \beta^m D_m K_{ij},\end{aligned} \tag{7}$$

where α is the lapse function, β_i the shift vector, and γ_{ij}, K_{ij}, and S_{ij} represent intrinsic metric, extrinsic curvature and stress tensor, respectively.

We express the matter with 5000 collisionless particles which move along the geodesic equation. For the lapse condition, we apply the maximal time slicing condition, so as not to hit a singularity in time evolution. We fix the shift vector as $\beta^i = 0$. We wrote our codes using the Cartesian coordinate.

Fig. 3 and 4 are snapshots of evolutions for the initial data $R_c = 0.70$ and 1.50, respectively. Both has no initial apparent horizons. We see the small radius ring immediately forms spheroidal apparent horizon soon after evolution starts, while the larger radius ring forms toroidal apparent horizon first and then forms common spheroidal horizon. The area of the horizons is always growing.

We searched both spheroidal and toroidal horizons simultaneously at every time step, but the switching of the horizon, from toroidal to spheroidal topology ($t = 1.12$ in the case of Fig. 4) is numerically clear.

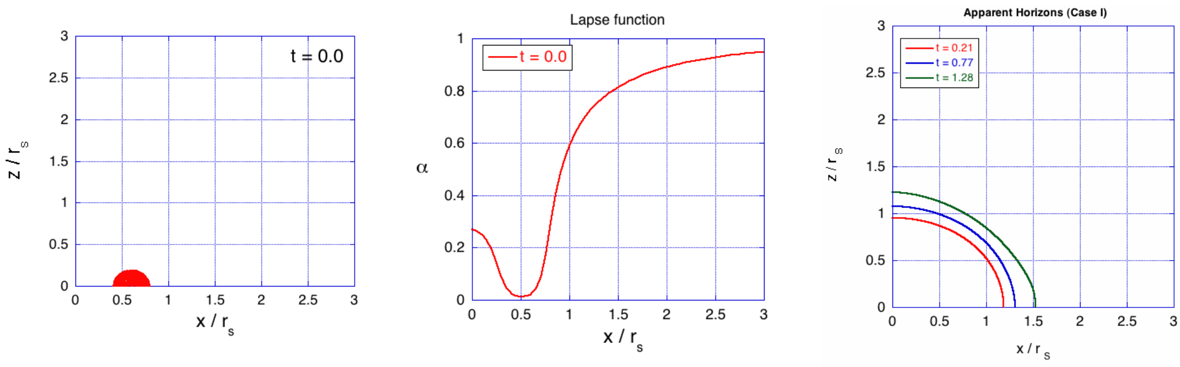

Figure 3: Snapshots of evolutions for the initial data $R_c = 0.70$ with no initial apparent horizon. (Left) Matter distributions at $t = 0$. (Center) lapse function, and (Right) the snapshots of the apparent horizons.

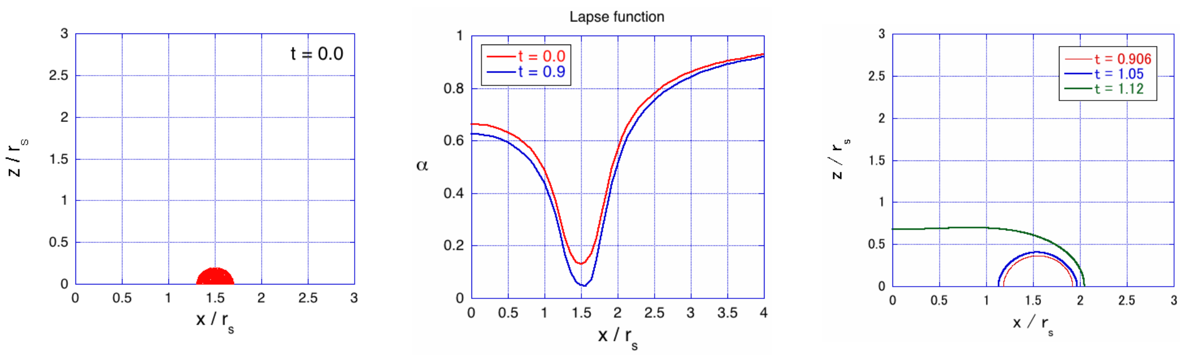

Figure 4: Snapshots of evolutions for the initial data $R_c = 1.5$ with no initial apparent horizon. (Left) Matter distributions at $t = 0$. (Center) lapse function, and (Right) the snapshots of the apparent horizons.

The current issues of our evolutions are (a) horizon finders, (b) slicing conditions, and (c) the set of evolution equations. (a) We confirmed the formation of the apparent horizons but not of the event horizons. The rigorous mathematical theorems denote that there is no toroidal event horizons in non-rotating space-time. Therefore we are developing event horizon finder to confirm the fact. (b) Since we are using the maximal slicing condition, the strong gravity region has quite small lapse function α so that there we can not see the actual time behaviors. We are planning to change the gauge condition to see further evolutions. (c) The set of ADM evolution equations is known to be unstable. The current simulations are only within initial stage of evolution, so that we are not facing the stability problem of the code. However, if we include the rotation of space-time, then evolution codes are required to follow longer dynamical behavior which might require us to change the set of evolution equations to somewhat adjusted or modified versions of ADM equations.

4 Summary

With a purpose of investigating the stability of black-ring solutions, we constructed initial-data of ring objects in five-dimensional spacetime. By searching apparent horizons and hyper-hoop, we verified the hyper-hoop conjecture and predict the time evolution. We also developed a code to follow the dynamics and showed initial time evolution.

For the analysis of initial data, we found that the shape of the apparent horizon switches from the common horizon to the ring horizon at a certain circle radius, and the former satisfies the hyper-hoop conjecture, while the latter is not. The area of the horizon and the thermo-dynamical analogy of black holes, imply the dynamical feature of the black-ring: a black-ring will naturally switch to a single black-hole. However, if the local gravity is strong, then the ring might begin collapsing to a ring singularity, that might produce also to the formation of 'naked ring' since $\mathcal{I}_{max}$ appears on the outside of the ring for a certain initial configuration.

We also investigate the dynamics of this initial data using collisionless particles under the maximal time slicing condition. We found the dynamical behaviors are different depending on the initial ring radius.

The initial-data sequences we showed here do not include rotations in matter and spacetime, so that those studies are our next subject. In the near future, we plan to report the stability of black-ring solutions.

This work was supported partially by the Grant-in-Aid for Scientific Research Fund of Japan Society of the Promotion of Science, No. 22540293. Numerical Computations were carried out on Altix3700 BX2 at YITP in Kyoto University and on the Riken Integrated Cluster of Clusters (RICC) at RIKEN.

References

[1] D. Ida and K. Nakao, Phys. Rev. D. **66**, 064026 (2002).

[2] C-M. Yoo, K. Nakao and D. Ida, Phys. Rev. D. **71**, 104014 (2005).

[3] R. Emparan and H. S. Reall, Phys. Rev. Lett. **88**, 101101 (2002).

[4] Y. Yamada and H. Shinkai, Class. Quant. Grav. **27**, 045012 (2010) [arXiv:0907.2570].

[5] N. O Murchadha and J. W. York, Jr., Phys. Rev. D. **10**, 428 (1974).

[6] S. L. Shapiro and S. A. Teukolsky, Phys. Rev. Lett. **66**, 994 (1991).

[7] M. Alcubierre, S. Brandt, B. Bruegmann, D. Holz, E. Seidel, R. Takahashi, J. Thornburg Int. J. Mod. Phys. **D10**, 273 (2001). [arXiv:gr-qc/9908012]